熱間鍛造により鉄基磁石材料の磁性向上
Enhancing the Magnetic Property of Nd-Lean Fe-based Alloy by Hot Forging Process

李　云平，劉　彬，高橋　弘紀，千葉　晶彦
東北大・金研
Y. Li[1], B. Liu[1], H. Takahashi, A. Chiba[1]
[1] Institute for Materials Research, Tohoku University

1. Introduction

Several processing routes for the production of Nd-Fe-B magnets have been developed since their elaboration in 1984. One of the major processing routes is based on powder metallurgy. In this method the mono-crystalline powder particles are aligned in a magnetic field with their c-axes of the tetragonal lattice parallel to each other. After pressing and sintering, an anisotropic magnet can be obtained, which exhibits high remanence (J_r) and maximum energy product ($(BH)_{max}$) [1]. High coercivity can be achieved in the ribbon flakes prepared by rapid solidification of molten alloy [2]. Appropriate combination of the alloy composition and processing parameters during sintering produce nano-crystalline or nano-composite (containing some proportion of soft magnetic phase) magnets [3, 4]. The enhanced magnetic properties evolve from the nano-crystalline structure of the Nd2Fe14B phase, which promotes magnetic exchange interactions [5]. The ribbon powder can further be processed to anisotropic magnet by hot working [6-8]. This procedure, developed by General Motors, comprises hot pressing of crushed powders into a fully dense isotropic bulk material followed by deformation such as hot extrusion, hot rolling or die-upset forging (hot pressing in an open die). As a result, the c-axes of the tetragonal cell of the Nd2Fe14B crystallites became parallel. Several approaches to the explanation of mechanisms leading to the anisotropy formation have been proposed. Li and Graham [9] suggested the mechanism based on dissolution of the non-favorably oriented crystallites in the Nd-rich phase and their re-precipitation on the crystallites, which have their c-axes oriented parallel to the stress direction. This idea was later supported by Leonowicz and Davies [10]. An extensive study was also carried out by Grünberger et al. [11]. He suggested a dominating role of the diffusion creep mechanism, which is also accompanied by rheological and viscous flow. Yuri and Ohki have made somewhat different approach [12]. Their model considers mechanical rotation of grains when they deform plastically and the alignment results from geometrical anisotropy of the crystallites. However, the above researches were basically based on the Nd-rich magnet. For Nd-lean magnet, detailed deformation mechanism is still unclear. The purpose of the present research is to clarify the detailed deformation mechanism of the Nd-Fe-B magnet (especially the Nd-lean Nd-Fe-B magnet) and to make clear the relationship among the processing, the dynamic recrystallization and the magnetic properties.

2. Experimental

Melt spun powders of Fe-10.9Nd-5.05B at. % were used in this study. The average particle size of the as-received powders is about 200μm. The melt spun powders were sintered at temperatures of 500°C-750°C. Figure 1 show the schematic diagram of the spark plasma sintering (SPS). Small cubes with edge of 2mm are cut from the sintered or deformed magnets for the magnetic properties measurements. The magnetic properties were measured parallel to the pressing direction. In order to investigate the influence of hot working process on the magnetic properties of Nd-Fe-B alloy, magnetic hysteresis loop measurements are planned to be performed using a vibrating sample magnetometer (VSM) with a max applied field of 15 Tesla.

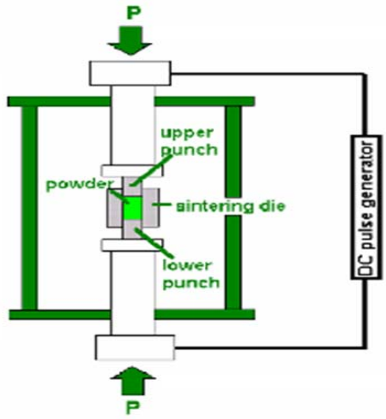

Figure 1. Schematic diagram of the spark plasma sintering.

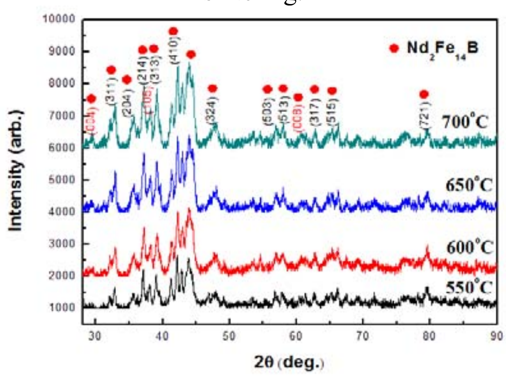

Figure 2 XRD patterns of the Fe-10.9Nd-5.05B compacts SPSed at temperature range of 500°C-750°C.

Figure 2 show the XRD patterns of Fe-10.9Nd-5.05B magnets sintered at temperatures from 550 °C to 700 °C.

It is clear that the peak widths are getting wider with increase the sintering temperature. All the samples exhibit only NdFeB main phase, no α phase can be identified from the XRD patterns. This is because of the low sintering temperature and short sintering time for the SPS sintering. Figure 3a and b show the SEM images (b is observed from the fracture surface) and Figure 9c shows the TEM image of the Fe-10.9Nd-5.05B magnet sintered at 700 °C. The sintered alloy exhibit a equiaxed microstructure with grain size of c.a. 65nm. The selection area diffraction (SAD) pattern confirms the existence of the nano-grains.

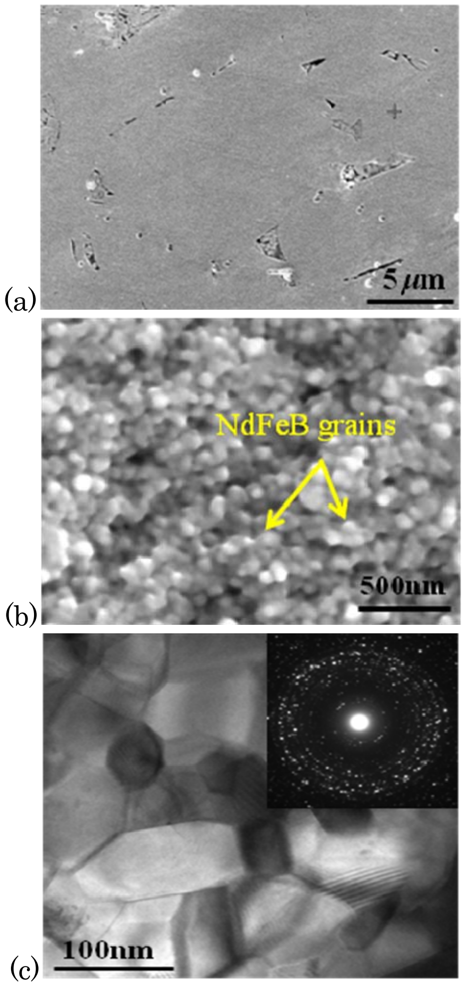

Figure 3 (a) SEM image, (b) Fracture surface and (c) TEM image of the Fe-10.9Nd-5.05B magnet sintered at 700°C.TEM image shows the nano-microstructure with average grain size of about 65nm.The embedded SAD pattern confirms the existence of the nano-grains.

Cylindrical compression specimens with size of d 8 × 10 mm^3 were cut from the SPSed compacts. Compressive tests were carried out in vacuum in the temperature range 1000–1200 °C and the strain rate range 0.001–10 s^{-1} using computer-aided Thermecmastor-Z equipment. The samples were first heated to the deformation temperature with speed of 3K/s, and then hold for 5min at those temperatures. After deformation, all specimens were quenched with a mixture of N_2 (6 MPa) and He (4 MPa) at a cooling rate of approximately 50 °C/s^{-1} in order to preserve the as-deformed microstructure.

Figure 4 shows the deformation curves at temperatures of 900°C and 1000°C and strain rates of 0.0003-0.1s^{-1}. All the curves show continuous work hardening, suggesting that the deformation mechanism is different from the traditional DRX and DRV where the deformation curves usually show flow softening.

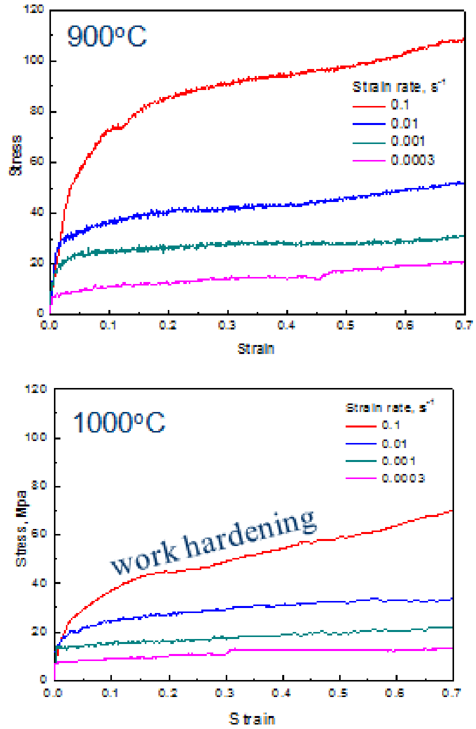

Figure 4 Ture strain-ture stress curves deformed at 900°C and 1000°C with different strain rates.

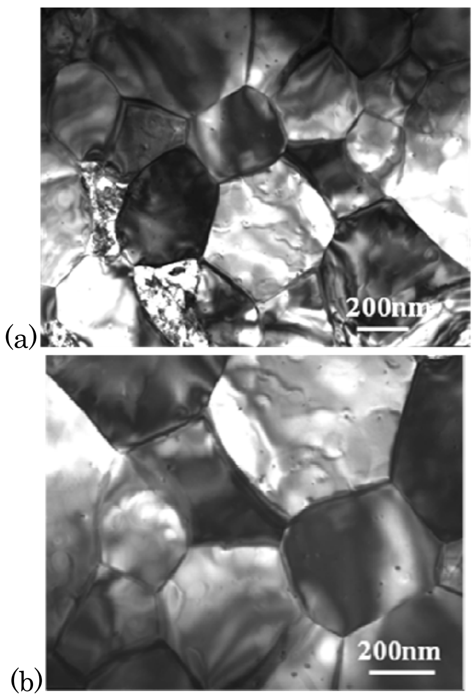

Figure 5 TEM images of the Fe-10.9Nd-5.05B magnet deformed at 800°C/0.01s^{-1}/50%.

Figure 5 shows the TEM images deformed at 800°C and strain rate of $0.01s^{-1}$. It is an equiaxed microstructure with grain size of 0.2-0.5μm. Dislocation microstructure is difficult to be identified in these TEM images, suggesting that the deformation mechanism should be the grain boundary sliding.

As the temperature increase to 1000°C and 1050°C, the grain size increase quickly, especially at 1050°C, the grain size increases to about 10μm. Deformation substructure is also hard to be found in the TEM image (Fig. 6). Figure 7 shows the magnetic properties of the Fe-10.9Nd-5.05B magnets before and after the deformation. It can be seen that after hot forging process obvious variation in the magnetic properties of materials occurred, implying the strong influence of hot forging on magnetic properties of this alloy.

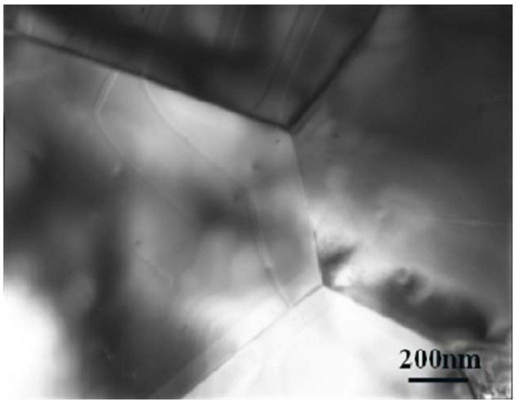

Figure 6 TEM images of the Fe-10.9Nd-5.05B sample deformed at $1050^{o}C/0.01s^{-1}/50\%$.

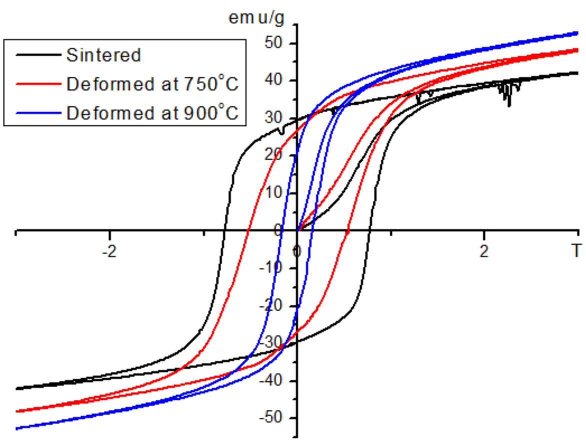

Figure7 Demagnetization curves of the Fe-10.9Nd-5.05B magnets before and after deformation

4. Conclusions

1. Nano-grained Nd-Fe-B magnets with average grain size of c.a. 50nm were successfully prepared through Melt-Spining+SPS process.
2. The nano-grained Nd-lean magnets show good deformability at temperature range of 850°C-1050°C and strain rate of $0.0003-0.1s^{-1}$. During deformation of the Nd-lean magnets, dislocation movement is hard to be observed. The deformation mechanism of the Nd-lean magnets is grain boundary sliding.
3. After hot forging process obvious variation in the magnetic properties of materials occurred, implying the strong influence of hot forging on magnetic properties of this alloy.

Reference

[1] S. Sagawa, F. Fujimura, M. Togawa, Y. Matsuura, J. Appl. Phys. 55 (1984) 2083.
[2] J.J. Croat, J.F. Herbst, R.W. Lee, F.E. Pinkerton, J. Appl. Phys. 50 (1984) 2078.
[3] J.E. Kem, G.B. Clemente, A.M. Kadin, R.W. McCallum, in: Proceedings of the Conference on ASM Materials Week'87, J.A. Salsgiver (Ed.) Am. Soc. Met. 1987, p. 87.
[4] H.A. Davies, A. Manaf, M. Leonowicz, Z.P.Z. Zhang, S.J. Dobson, R.A. Buckley, Nanostruct. Mater. 2 (1993) 197.
[5] G. Hertzer, IEEE Trans. Magn. 26 (1990) 1397.
[6] J.J. Croat, J.F. Herbst, R.W. Lee, F.E. Pinkerton, J. Appl. Phys. 50 (1984) 2078.
[7] R.W. Lee, Appl. Phys. Lett. 46 (1985) 790.
[8] T. Shimoda, K. Akioka, O. Kobayashi, T. Yamagami, IEEE Trans.Magn. 25 (1989) 4099.
[9] Lin Li, C.D. Graham Jr., IEEE Trans. Magn. 28 (1992) 2130.
[10] M. Leonowicz, H.A. Davies, Mater. Lett. 19 (1994) 275.
[11] W. Grünberger, D. Hintz, A. Kirchner, K.H. Müller, L. Schultz, J.Alloys Compd. 257 (1997) 293.
[12] T. Yuri, T. Ohki, in: Proceedings of the 13th International Workshop on Rare Earth Magnets and their Applications, Birmingham, 11-14 September, 1994, p. 645.